Available online at www.sciencedirect.com

ScienceDirect

Journal of Differential Equations 374 (2023) 632–641

Journal of Differential Equations

www.elsevier.com/locate/jde

A steady azimuthal stratified flow modelling the Antarctic Circumpolar Current

A.A. Abrashkin [a,b], A. Constantin [c,*]

[a] *Department of Mathematics, National Research University Higher School of Economics, 603155 Nizhny Novgorod, Russia*

[b] *Federal Research Center, Institute of Applied Physics of the Russian Academy of Sciences, Nizhny Novgorod, Russia*

[c] *Faculty of Mathematics, University of Vienna, Oskar-Morgenstern-Platz 1, 1090 Vienna, Austria*

Received 15 February 2023; revised 22 July 2023; accepted 27 July 2023

Abstract

We investigate steady flow moving purely in the azimuthal direction on a rotating sphere and having a meridionally localized jet structure. An exact solution for a stratified inviscid fluid, which admits a depth-dependent velocity profile below the surface, is constructed in spherical coordinates. This solution is relevant to the modelling of the Antarctic Circumpolar Current. We show that the stratification enables us to dispense with the nonconservative body force that was invoked in recent spherical-coordinate models to produce realistic flow profiles.

MSC: 86A05; 35Q35

Keywords: Stratified fluid; Inviscid flow

1. Introduction

The wind-driven Antarctic Circumpolar Current (ACC) is the only ocean current to close upon itself in a circumpolar loop [8,23]. The ACC is crucial to the Earth's climate because its vast zonal transport links the southern regions of the Atlantic, Pacific and Indian Oceans (see

* Corresponding author.

E-mail addresses: aabrashkin@hse.ru (A.A. Abrashkin), adrian.constantin@univie.ac.at (A. Constantin).

https://doi.org/10.1016/j.jde.2023.07.044

Fig. 1), mixing the water between these basins and thus enabling a global ocean circulation. The ACC's continuous nearly-zonal band of eastward flow, largely between 40°S–60°S, effectively isolates the Antarctic continent from the tropical regions, thus contributing toward making it the coldest place on Earth. The narrowest constriction to the flow of the ACC is Drake Passage (about 700 km across, at the southern tip of South America), but away from it the ACC is typically 2000 km wide. In contrast to other major ocean currents, the ACC is not a single flow but a fragmented system consisting of several high-speed, vertically coherent, seafloor-reaching jets, separated by zones of low-speed currents. The magnitude of the ACC's zonal flow component greatly exceeds its meridional component, with the vertical velocity overall negligible. ACC currents extend throughout the water column, declining monotonically with depth from a mean surface speed of about 20 $\mathrm{cm\,s^{-1}}$ to a few $\mathrm{cm\,s^{-1}}$ near the bottom [12]. The fastest jet is the subantarctic front, marking the northern boundary of the ACC (see Fig. 1), with speeds in excess of 1 $\mathrm{m\,s^{-1}}$. The primary source of momentum for the ACC is wind stress imparted by some of the strongest winds on the planet – the persistently strong westerly winds, punctuated by frequent gales, led sailors to christen the southern latitudes the roaring forties, furious fifties and screaming sixties. The fact that the ACC currents reach the 4 km deep sea floor is a result of the weak stratification in the Southern Ocean and of a pressure gradient force that is quite evenly distributed over the water column, due to the combined effect of consistently large wind speeds with little variation in wind direction [22].

The ACC flow is nearly zonal, practically following a circle of latitude in the regions of the abyssal plains of the Southern Ocean, located in the three major basins where the depth exceeds 4 km (the Pacific-Antarctic Basin, the Australian-Antarctic Basin in the Indian Ocean sector, and the Atlantic-Indian Basin). However, some bottom topography features of the Southern Ocean with scales similar to terrestrial mountain ranges and spanning distances of the order of 1000 km have a significant effect on steering the path of the seafloor-reaching ACC flow [17]:

- a sharp northward shift is caused by the 2 km deep Scotia Ridge (between 55° and 40° W, downstream of South America), formed by continental fragments that once formed a land bridge between South America and Antarctica, and containing numerous islands;
- poleward shifts occur at the Southwest Indian Ridge (between 20° and 30°E) and through the fracture zones in the Pacific-Antarctic Ridge (between 145° and 120° W), the average water depth to the top of these ridges being 2.5 km and 3 km, respectively;
- the ACC's continuous nearly-zonal band of eastward flow widens in the southwestern Indian Ocean due to the obstruction of the 3 km deep Kerguelen Plateau near 70°E, but no significant departure of the current direction across the plateau is observed [22].

In light of the above descriptions of the flow pattern of the ACC, it is of interest to derive exact solutions to the nonlinear governing equations for steady ocean flow moving purely in the azimuthal direction and having a meridionally localized jet structure. While exact solutions are rare and capture only partly the inherent complexity of physical phenomena, they are precise in their validity and offer detailed insight into basic features of the flow pattern. Exact solutions are also a useful starting point for a perturbation analysis. Current advances in computing enhance the feasibility of numerical simulations of perturbed flows that can capture a wider range of effects, whose importance can be ascertained by comparison with the exact solutions. Nonlinearity is considered to be inherent to the ACC flow and from the perspective of perturbation theory it is desirable to incorporate nonlinear effects already at leading order, rather than merely as perturbations of a linear background flow.

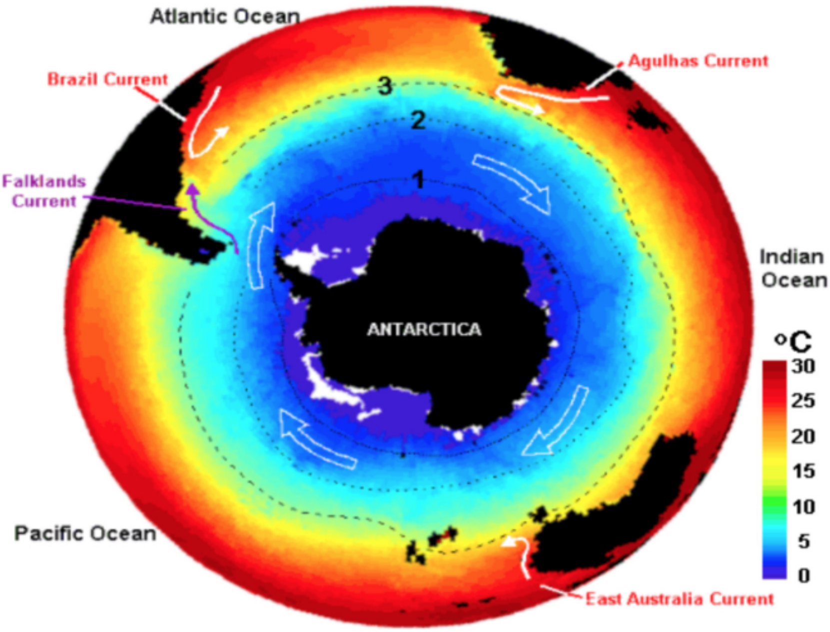

Fig. 1. Satellite image (courtesy of NASA's SeaWiFS project) of sea surface temperature revealing two main jets of the eastward flowing ACC: 1) the polar front, 2) the subantarctic front. Overall there are nine circumpolar jets, each about 50 km wide [16]. The subtropical front, marked 3), is the northern boundary of the Southern Ocean but is not circumpolar, its path being interrupted by South America.

Given the specific features of the ACC, it is advantageous to use spherical coordinates rather than performing f-plane or β-plane approximations that impose flat-space geometry – see also the discussion in [6]. Recently, exact solutions in spherical coordinates were presented in [3,5,10] for equatorial flows. More importantly, such solutions for the ACC were obtained in [4] under the simplifying assumption of constant density, hypothesis motivated by the weak stratification of the Southern Ocean. However, in the constant-density setting a nonconservative body force has to be invoked to produce realistic flow profiles – see also [11,14] for related investigations. We will show that accounting for stratification (incorporating the effects of temperature, salinity and depth on the variations of the density by means of an adequate equation of state) enables us to dispense with this additional assumption. With regard to the alternative nonlinear gyre models of the ACC that were pursued recently in [1,9,15], note that the gyre approach, which requires comparable orders of magnitude for the zonal and meridional velocity components and does not incorporate depth-dependence, is only adequate for the near-surface ocean flow.

The plan of the paper is to outline in Section 2 the problem in rotating spherical coordinates, by presenting the nonlinear equations to which the governing equations reduce for steady ocean flow moving purely in the azimuthal direction and having a meridionally localized jet structure. In Section 3 we derive the general exact solution for a realistic stratification. We conclude with a discussion of the flow features of the ACC that are highlighted by means of the structural properties of the exact solutions that were obtained in this paper.

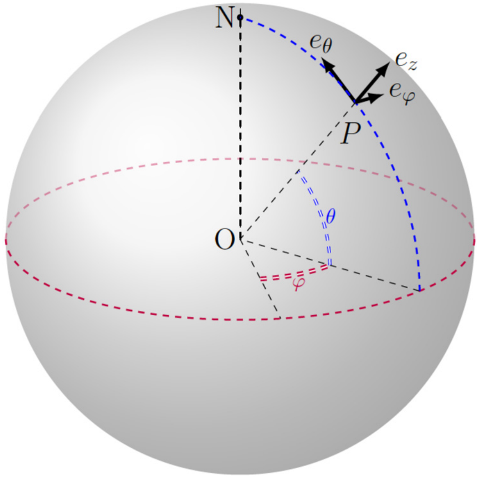

Fig. 2. The rotating spherical coordinate system, where θ is the angle of latitude,   is the azimuthal angle and $r' = |\mathbf{r}'|$ is the distance from the origin at the Earth's centre. The North/South Poles are at $\theta = \pm\pi/2$ and the Equator is on $\theta = 0$, while the Antarctic Circumpolar Current sits at about $\theta = -\pi/4$.

2. Formulation of the problem

Since the ACC envelopes entire latitude circles, it is adequate to use spherical coordinates rather than the f-plane or β-plane setting. We introduce a set of (right-handed) spherical coordinates, $(\ \ , \theta, r)$: r is the distance (radius) from the centre of the sphere, $\theta \in (-\pi/2, \pi/2)$ is the angle of latitude and $\ \ \in [0, 2\pi)$ is the azimuthal angle i.e. the angle of longitude, measured with respect to the prime meridian (see Fig. 2). The unit vectors in this $(\ \ , \theta, r)$-system, for all points but the two poles (where $\mathbf{e}\ \ $ and $\mathbf{e}_\theta$ are not well-defined, an unavoidable feature since the sphere does not possess a continuously differentiable field of unit tangent vectors – see the discussion in [2]), are $(\mathbf{e}\ \ , \mathbf{e}_\theta, \mathbf{e}_r)$, respectively, and the corresponding velocity components are (u, v, w), with $\mathbf{e}\ \ $ pointing from West to East, $\mathbf{e}_\theta$ from South to North and $\mathbf{e}_r$ upwards (see Fig. 2). The $(\ \ , \theta, r)$-system is associated with a point fixed on the sphere which is rotating about its polar axis (with an angular speed $\Omega' \approx 7.29 \times 10^{-5}$ rad s^{-1}).

We consider an inviscid stratified ocean flow. The Euler equation and the equation of mass conservation are, respectively,

$$\begin{aligned}&\Big(\frac{\partial}{\partial t} + \frac{u}{r\cos\theta}\frac{\partial}{\partial \ } + \frac{v}{r}\frac{\partial}{\partial\theta} + w\frac{\partial}{\partial r}\Big)(u, v, w) + \frac{1}{r}(-uv\tan\theta + uw, u^2\tan\theta + vw, -u^2 - v^2)\\ &\quad + 2\Omega\,(-v\sin\theta + w\cos\theta, u\sin\theta, -u\cos\theta) + r\Omega^2\,(0, \sin\theta\cos\theta, -\cos^2\theta)\\ &= -\frac{1}{\rho}\Big(\frac{1}{r\cos\theta}\frac{\partial p}{\partial \ }, \frac{1}{r}\frac{\partial p}{\partial\theta}, \frac{\partial p}{\partial r}\Big) + (0, 0, -g)\,, \end{aligned} \tag{2.1}$$

and

$$\frac{\partial\rho}{\partial t} + \frac{u}{r\cos\theta}\frac{\partial\rho}{\partial \ } + \frac{v}{r}\frac{\partial\rho}{\partial\theta} + w\frac{\partial\rho}{\partial r} + \rho\Big\{\frac{1}{r\cos\theta}\frac{\partial u}{\partial \ } + \frac{1}{r\cos\theta}\frac{\partial}{\partial\theta}(v\cos\theta) + \frac{1}{r^2}\frac{\partial}{\partial r}(r^2 w)\Big\} = 0\,, \tag{2.2}$$

where t is time, $p(\ ,\theta,r,t)$ is the pressure and $\rho(\ ,\theta,r,t)$ the density, with $g=\text{constant}\approx 9.81$ m s^{-2}, a reasonable choice for the depths of the oceans on Earth.

At the free surface, $r=R+h(\theta,\ )$, where $R\approx 6378$ km is the (mean) radius of the Earth, we impose a surface pressure and the kinematic boundary condition:

$$p=P(\ ,\theta) \quad \text{on} \quad r=R+h(\ ,\theta)\,, \tag{2.3}$$

and

$$w=\frac{u}{r\cos\theta}\frac{\partial h}{\partial\ }+\frac{v}{r}\frac{\partial h}{\partial\theta} \quad \text{on} \quad r=R+h(\ ,\theta)\,, \tag{2.4}$$

respectively. At the bottom of the ocean, $r=R+d(\ ,\theta)$, which we take to be an impermeable, solid boundary, we have the corresponding kinematic boundary condition:

$$w=\frac{u}{r\cos\theta}\frac{\partial d}{\partial\ }+\frac{v}{r}\frac{\partial d}{\partial\theta} \quad \text{on} \quad r=R+d(\ ,\theta)\,. \tag{2.5}$$

We investigate a steady flow propagating purely in the azimuthal direction, with a flat free surface over a flat bed, so $h=h_0>0$ (constant), $d=0$ and $v=w=0$ throughout the relevant ocean region. Further, this flow does not vary in the azimuthal direction, so $u=u(r,\theta)$, with $p=p(r,\theta)$, $P=P(\theta)$ and $\rho=\rho(r,\theta)$. The equation of mass conservation (2.2) and the kinematic boundary conditions (2.4)–(2.5) are now satisfied, with the equations of fluid motion (2.1) taking the form

$$\frac{u^2}{r}\tan\theta+2\Omega u\sin\theta+r\Omega^2\sin\theta\cos\theta=-\frac{1}{\rho r}\frac{\partial p}{\partial\theta}\,, \tag{2.6}$$

$$-\frac{u^2}{r}-2\Omega u\cos\theta-r\Omega^2\cos^2\theta=-\frac{1}{\rho}\frac{\partial p}{\partial r}-g\,, \tag{2.7}$$

in the region $R<r<R+h_0$, and with the surface pressure condition (2.3) simplifying to

$$p=P(\theta) \quad \text{on} \quad r=R+h_0\,. \tag{2.8}$$

The seawater density ρ is governed by temperature T, salinity and depth r. The salinity of the Southern Ocean ranges from 34 to 35 ppt, with sea-surface values decreasing with the distance to the South Pole, being predominantly influenced by the sea-ice cover and by thawing icebergs (see [7]). Also, the temperature variations are rather small – the difference between the surface and the bottom water does not exceed 4 °C, about 20% of the difference found in tropical regions (see [22]). For these reasons, the depth is the main stratification factor and it is adequate to consider the following form of the equation of state:

$$\rho=\rho(T,\ ,r)\approx\rho_0(r)-\alpha(T-T_0)+\beta(\ -\ _0)\,, \tag{2.9}$$

where T_0 and $_0$ are mean surface values, $\alpha\approx 53\times 10^{-3}$ kg K^{-1} m^{-3} is the thermal expansion coefficient multiplied by the average density and $\beta\approx 785\times 10^{-3}$ kg m^{-3} is the saline contraction coefficient [20]. Since the water density varies between 1026 and 1028.5 kg m^{-3}, (2.10) captures

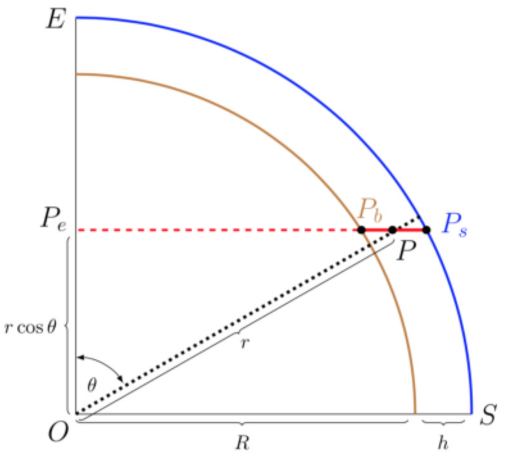

Fig. 3. Sketch of the invariance of the velocity profile for a homogeneous ocean; O marks the centre of the spherical Earth, E the position of the Equator and S the South Pole. The free surface of the ocean is drawn in blue, the bed in brown, and P is a point in the Southern Ocean, at latitude θ and depth $r-(R+d)$. The line through P parallel to the polar axis intersects the equatorial plane in P_e, the ocean bed in P_b and the ocean surface in P_s, with the velocity u constant along the segment P_bP_s due to (3.6) for constant density ρ.

the fact that the density variation is mainly due to depth changes. The distributions of temperature and salinity across the ACC reveal the characteristic southward upward tilt of surfaces parallel to the polar axis (see Fig. 3) on which the values of certain physical characteristics are nearly uniform [12,13]. We therefore consider the density distribution

$$\rho = \rho_0(r) + \gamma r \cos\theta\,, \tag{2.10}$$

where ρ_0 is a decreasing function and $\gamma > 0$ is a constant.

3. General solution

Expressing

$$\begin{aligned} u(r,\theta) &= f(r,s) \\ p &= F(r,s) \end{aligned} \qquad \text{with} \quad s = r\cos\theta\,, \tag{3.1}$$

in the latitude band $\theta \in [-40^\circ, -60^\circ]$ (to which the Antarctic Circumpolar Current is confined) and for $r \in [R, R+h_0]$ (corresponding to the depth range of the Southern Ocean), we transform the equations (2.6)-(2.7) into

$$\frac{\partial F}{\partial s} = \frac{\rho}{s}\,(f+\Omega s)^2\,, \tag{3.2}$$

$$\frac{\partial F}{\partial r} = -\,\rho g\,, \tag{3.3}$$

in the region $R < r < R + h_0$. From (2.10) and (3.3) we get

$$F(r,s)=g\int_r^{R+h_0}\rho_0(r')\,\mathrm{d}r'-\gamma sr+A(s) \tag{3.4}$$

with the surface pressure condition (2.8) specifying

$$A(s)=P\Big(\arccos\Big(\frac{s}{R+h_0}\Big)\Big)+\gamma(R+h_0)s\,,\qquad s\in\big[\tfrac{1}{2}(R+h_0),\,(R+h_0)\cos(40^\circ)\big]. \tag{3.5}$$

From (3.4) and (3.2) we now obtain

$$f(r,s)=-s\Omega+\sqrt{\frac{s\big(\frac{\mathrm{d}A}{\mathrm{d}s}(s)-\gamma r\big)}{\rho_0(r)+\gamma s}}\,,\qquad (r,s)\in[R,R+h_0]\times\big[\tfrac{1}{2}R,\,(R+h_0)\cos(40^\circ)\big]. \tag{3.6}$$

This completes the derivation of the general solution to the system (2.6)-(2.7) for a density distribution of the form (2.10). Note that the values of $A(s)$ for $s\in\big[\frac{1}{2}R\,,\,\frac{1}{2}(R+h_0)\big)$ are not specified, so that we have a large family of exact solutions. The only constraint that has to be imposed on the definition of the function A on the interval $\big[\frac{1}{2}R\,,\,\frac{1}{2}(R+h_0)\big)$ is

$$\frac{\mathrm{d}A}{\mathrm{d}s}(s)>\gamma r+\Omega^2 s[\rho_0(r)+\gamma s]\,, \tag{3.7}$$

to ensure an eastward flow. The inequality (3.7) has also to hold for $s\in\big[\frac{1}{2}(R+h_0),\,(R+h_0)\cos(40^\circ)\big]$. Setting $r=R+h_0$ in the relation

$$\frac{\mathrm{d}A}{\mathrm{d}s}=-\frac{s\,\frac{\mathrm{d}P}{\mathrm{d}\theta}(\theta)}{\sqrt{(R+h_0)^2-s^2}}+\gamma(R+h_0)\,,$$

ensured by (3.5), this can only be the case if the sea level pressure throughout the latitude band of the ACC increases with the distance to the South Pole, a feature confirmed by field data (see [19]).

3.1. The constant density assumption

For constant density $\rho=\rho_0$ (constant) the general solution (3.6) simplifies to

$$u(r,\theta)=-s\Omega+\frac{\sqrt{-r\cos\theta\,\frac{\mathrm{d}P}{\mathrm{d}\theta}(\theta)}}{\sqrt{\rho_0}\,[(R+h_0)^2-r^2\cos^2\theta]^{1/4}}\,, \tag{3.8}$$

with the associated pressure given by the corresponding simplification

$$p(r,\theta)=g\rho_0(r-R-h_0)+P\Big(\arccos\Big(\frac{r\cos\theta}{R+h_0}\Big)\Big)\,, \tag{3.9}$$

of (3.4)-(3.5). The solution (3.8) is not realistic since along any arc of fixed latitude the zonal velocity u is constant on the lines $r\cos\theta=$ constant, which are parallel to the polar axis of rotation: this is equivalent to the Taylor-Proudman theorem [21,18]. In this setting, the maximal speed would be attained at the ocean bed (see Fig. 3), which is in severe contradiction to physical reality. To address this shortcoming, the approach in [4] invoked an additional nonconservative forcing whose exact nature is however debatable (relevant factors might be turbulent fluxes and the topographic form drag). Accounting for stratification destroys this alignment property and permits us to obtain realistic flow profiles by means of formula (3.6) with $\gamma > 0$ and a strictly decreasing function $r \mapsto \rho_0(r)$ on $[R, R+h_0]$. We now discuss two examples, based on different choices for the surface pressure in (2.8) as a polynomial expression in $\cos\theta$. As pointed out in the derivation of the general solution formulae (3.4) and (3.6), these choices are subject to the constraint $\dfrac{\mathrm{d}P}{\mathrm{d}\theta}(\theta) < 0$.

3.2. A simple particular solution

To obtain a simple physically relevant flow pattern we choose the surface pressure of the form

$$P(\theta) = P_0 + P_1 \cos\theta$$

with $P_0,\ P_1 > 0$ constants. In view of (3.4), we set

$$A(s) = P_0 + ks \quad \text{with} \quad k = \frac{P_1}{R+h_0} + \gamma(R+h_0)\,,$$

obtaining from (3.1) and (3.6) the zonal fluid velocity

$$u(r,\theta) = -\Omega r\cos\theta + \sqrt{\frac{(k-\gamma r)r\cos\theta}{\rho_0(r)+\gamma r\cos\theta}}\,, \tag{3.10}$$

that does not vanish at the flat bed $r = R$.

3.3. A zonal flow vanishing at the flat bed

We now show that an adequate choice of the surface pressure of the form

$$P(\theta) = P_0 + P_1\cos\theta + P_2\cos^2\theta + P_3\cos^3\theta$$

with $P_0,\ P_1,\ P_2,\ P_3 > 0$ suitable constants, produces a flow that does not reach the bed. Taking (3.4) into account, we set

$$\begin{aligned} &A(s) = P_0 + k_1 s + k_2 s^2 + k_3 s^3 \\ &\text{with} \quad k_3 = \frac{P_3}{(R+h_0)^3}\,, \quad k_2 = \frac{P_2}{(R+h_0)^2}\,, \quad k_1 = \frac{P_1}{R+h_0} + \gamma(R+h_0)\,, \end{aligned}$$

so that (3.1) and (3.6) yield the associated zonal fluid velocity

$$u(r,\theta) = -\Omega r\cos\theta + \sqrt{\frac{(k_1-\gamma r+2k_2 r\cos\theta+3k_3r^2\cos^2\theta)r\cos\theta}{\rho_0(r)+\gamma r\cos\theta}}\,. \tag{3.11}$$

Consequently, the zonal flow along the flat bed $r = R$ vanishes if

$$P_1 = \gamma R(R+h_0) - \gamma (R+h_0)^2\,, \quad P_2 = \tfrac{1}{2}\,\rho_0(R)\Omega^2 R(R+h_0)^2\,, \quad P_3 = \tfrac{1}{3}\,\gamma\,\Omega^2 R^2 (R+h_0)^3\,.$$

4. Discussion

The presented analysis provides us with an exact zonal solution to the full set of nonlinear governing equations for inviscid ocean flow in rotating spherical coordinates. The fact that the Reynolds stresses and viscous terms are very small for the ACC flow permits us to use this exact solution as a model for the background pure current flow of the ACC: the solution describes a zonal current that is not restricted to a near-surface layer but extends to great depths (down to the ocean floor). In contrast to the classical theory of free-surface water flows, which assumes constant atmospheric pressure at the ocean surface, for this wind-drift current we allow meridional sea-surface pressure changes, with a pressure that decreases as the latitude increases – a feature suggested by field data. The examples presented in Section 3.2 and 3.3 show that the exact nature of this change is related to whether the current reaches the seafloor or not. An important role in our considerations is played by stratification. The weak stratification of the Southern Ocean is nevertheless dynamically important since, as shown in Section 3.1, the constant density assumption would produce flows that are not physically realistic. The multitude of jets associated to the ACC can be investigated within the proposed setting simply by combining a number of zonal currents of the type described in Section 3.

The practical benefit of an analytically tractable model of the ACC is that the very fact that it represents a simplified version of an inherently complex flow makes it possible to reveal the dominant features of the overall dynamics. Exact solutions serve also as a test case for numerical models and open up the possibility of a perturbative approach. The solution described in this paper is to be regarded as a background pure current flow enabling future in-depth studies of wave-current interactions, in the form of wave perturbations of this background state to be investigated by means of an interactive exploration of analytical approaches and numerical simulations.

Data availability

All data for this paper are properly cited and referred to.

Acknowledgments

This research was supported by the Grant Z 387-N of the Austrian Science Fund (FWF). The authors are grateful for helpful comments from the referee. All data used in this paper are to be found in [7,12,13,16,17,19,20,22].

References

[1] J. Chu, K. Marynets, Z. Wang, Existence and approximate solutions of a nonlinear model for the Antarctic Circumpolar Current, Differ. Integral Equ. 36 (2023) 537–558.

[2] A. Constantin, P. Germain, An exact, steady, purely azimuthal equatorial flow with a free surface, Arch. Ration. Mech. Anal. 245 (2022) 587–644.

[3] A. Constantin, R.S. Johnson, An exact, steady, purely azimuthal equatorial flow with a free surface, J. Phys. Oceanogr. 46 (2016) 1935–1945.

[4] A. Constantin, R.S. Johnson, An exact, steady, purely azimuthal flow as a model for the Antarctic Circumpolar Current, J. Phys. Oceanogr. 46 (2016) 3585–3594.

[5] A. Constantin, R.S. Johnson, On the nonlinear, three-dimensional structure of equatorial oceanic flows, J. Phys. Oceanogr. 49 (2019) 2029–2042.

[6] A. Constantin, R.S. Johnson, Steady large-scale ocean flows in spherical coordinates, Oceanography 31 (2018) 42–50.

[7] E. Garcia-Eidell, J.D. Comiso, E. Dinnat, L. Brucker, Sea surface salinity distribution in the Southern Ocean as observed from space, J. Geophys. Res., Oceans 124 (2019) 3186–3205.

[8] A.E. Gill, Atmosphere-Ocean Dynamics: An Introductory Text, Academic Press, 1982.

[9] S.V. Haziot, K. Marynets, Applying the stereographic projection to modeling of the flow of the Antarctic Circumpolar Current, Oceanography 31 (2018) 63–75.

[10] D. Henry, C.I. Martin, Exact, free-surface equatorial flows with general stratification in spherical coordinates, Arch. Ration. Mech. Anal. 233 (2019) 497–512.

[11] D. Ionescu-Kruse, Local stability for an exact steady purely azimuthal flow which models the Antarctic Circumpolar Current, J. Math. Fluid Mech. 20 (2018) 569–579.

[12] J. Klinck, W.D. Nowlin, Southern Ocean–Antarctic Circumpolar Current, in: J. Steele, S. Thorpe, K. Turekian (Eds.), Encyclopedia of Ocean Sciences, Academic Press, San Diego, 2001, pp. 151–159.

[13] J. Marshall, K. Speer, Closure of the meridional overturning circulation through Southern Ocean upwelling, Nat. Geosci. 5 (2012) 171–180.

[14] C.I. Martin, R. Quirchmayr, Exact solutions and internal waves for the Antarctic Circumpolar Current in spherical coordinates, Stud. Appl. Math. 148 (2022) 1021–1039.

[15] K. Marynets, The Antarctic Circumpolar Current as a shallow-water asymptotic solution of Euler's equation in spherical coordinates, Deep-Sea Res. 160 (2019) 58–62.

[16] E.G. Morozov, D.I. Frey, D.V. Fofanov, V.A. Krechik, R.Yu. Tarakanov, D.L. Vinokurov, The extreme northern jet of the Antarctic Circumpolar Current, Rus. J. Earth Sci. 20 (2020) 58–62.

[17] R.D. Patmore, R.R. Holland, D.R. Munday, A.C. Naveira Garabato, D.P. Stevens, M.P. Meredith, Topographic control of Southern Ocean gyres and the Antarctic Circumpolar Current: a barotropic perspective, J. Phys. Oceanogr. 49 (2019) 3221–3244.

[18] J. Proudman, On the motions of solids in a liquid possessing vorticity, Proc. R. Soc. Lond. A 92 (1916) 408–424.

[19] N.A. Romanova, P.Yu. Romanov, Antarctic wind intensification as inferred from the NCEP/NCAR reanalysis data, J. Oceanol. Res. 48 (2020) 96–108.

[20] L.D. Talley, G.L. Pickard, W.J. Emery, J.H. Swift, Descriptive Physical Oceanography: An Introduction, Elsevier, Amsterdam, 2011.

[21] G.I. Taylor, Motions of solids in fluids when the flow is not irrotational, Proc. R. Soc. Lond. A 93 (1917) 92–113.

[22] M. Tomczak, J.S. Godfrey, Regional Oceanography: An Introduction, Daya Publ., Delhi, 2003.

[23] G.K. Vallis, Atmospheric and Oceanic Fluid Dynamics, Cambridge University Press, 2017.